Journal of Physics and Chemistry of Solids 72 (2011) 761–767

Contents lists available at ScienceDirect

Journal of Physics and Chemistry of Solids

journal homepage: www.elsevier.com/locate/jpcs

Derivation of the optical constants of spin coated CeO_2–TiO_2–ZrO_2 thin films prepared by sol–gel route

F.E. Ghodsi [a,*], F.Z. Tepehan [b], G.G. Tepehan [c]

[a] Department of Physics, Faculty of Science, The University of Guilan, Namjoo Ave., P.O. Box 41335-1914, Rasht, Iran
[b] Department of Physics, Faculty of Sciences and Letters, Istanbul Technical University, Maslak, Istanbul 34469, Turkey
[c] Faculty of Arts and Sciences, Kadir Has University, Cibali, Istanbul 34083, Turkey

ARTICLE INFO

Article history:
Received 22 June 2010
Received in revised form
6 March 2011
Accepted 16 March 2011
Available online 8 April 2011

Keywords:
A. Thin films
D. Optical properties

ABSTRACT

Ternary thin films of cerium titanium zirconium mixed oxide were prepared by the sol–gel process and deposited by a spin coating technique at different spin speeds (1000–4000 rpm). Ceric ammonium nitrate, $Ce(NO_3)_6(NH_4)_2$, titanium butoxide, $Ti[O(CH_2)_3CH_3]_4$, and zirconium propoxide, $Zr(OCH_2CH_2CH_3)_4$, were used as starting materials. Differential calorimetric analysis (DSC) and thermogravimetric analysis (TGA) were carried out on the CeO_2–TiO_2–ZrO_2 gel to study the decomposition and phase transition of the gel. For molecular, structural, elemental, and morphological characterization of the films, Fourier Transform Infrared (FTIR) spectral analysis, X-ray diffraction (XRD), energy dispersive X-ray spectroscopy (EDS), cross-sectional scanning electron microscopy (SEM), and atomic force microscopy (AFM) were carried out. All the ternary oxide thin films were amorphous. The optical constants (refractive index, extinction coefficient, band gap) and thickness of the films were determined in the 350–1000 nm wavelength range by using an nkd spectrophotometer. The refractive index, extinction coefficient, and thickness of the films were changed by varying the spin speed. The oscillator and dispersion energies were obtained using the Wemple–DiDomenico dispersion relationship. The optical band gap is independent of the spin speed and has a value of about $E_g \approx 2.82 \pm 0.04$ eV for indirect transition.

1. Introduction

Over the past decades, many kinds of deposition techniques have been developed in thin film production technology. Some of these techniques are effective, but they are also expensive and may need high temperatures for the deposition process [1–3]. The sol–gel process is an economical and energy saving deposition method capable of preparing high quality metal oxide thin films over large area and at low temperatures [4,5]. Metal oxide formed in thin films with tailored physical properties is of interest for applications in optics, sensors, electrochromic devices, and protective coatings as well as in microelectronics and optoelectronics [6–8]. In recent years, CeO_2, binary CeO_2–TiO_2, and CeO_2–ZrO_2, and ternary CeO_2–TiO_2–ZrO_2 thin films have received significant attention due to their interesting ion storage properties, which make them very attractive for electrochromic applications [9–12]. However, to our knowledge, there has been no thorough study of ternary CeO_2–TiO_2–ZrO_2 thin films using spin coating techniques. This paper reports on preparation of such spin-coated films by using the sol–gel process. The decomposition and phase transition of the gel were measured by Differential calorimetric analysis (DSC) and thermogravimetric analysis (TGA). The structure of such films has been characterized by X-ray diffraction (XRD). Atomic Force Microscopy (AFM) and cross-sectional scanning electron microscopy (SEM) images were prepared to correlate optical properties and morphology of the CeO_2–TiO_2–ZrO_2 thin films. The molecular and elemental properties of samples were carried out by Fourier Transform Infrared (FTIR) spectral analysis and energy dispersive X-ray spectroscopy (EDS). The optical constants and film thickness were derived from transmittance-reflectance spectra of the films by nkd spectrophotometer. The aim of this report is to show the correlations between spinning rate and the optical and morphological properties of the sol–gel derived CeO_2–TiO_2–ZrO_2 thin films.

2. Experimental method

2.1. Solution preparation and deposition procedure

A precursor solution was prepared by dissolving $Ce(NO_3)_6(NH_4)_2$ (CEAMN) in C_2H_5OH (EtOH) and stirred for 30 min. Then, $Ti[O(CH_2)_3CH_3]_4$ ($Ti(OBU)_4$), and $Zr(OCH_2CH_2CH_3)_4$ ($Zr(OP)_4$) were

* Corresponding author. Tel.: +98 1313223031; fax: +98 1313220066.
E-mail address: feghodsi@guilan.ac.ir (F.E. Ghodsi).

0022-3697/$ - see front matter © 2011 Published by Elsevier Ltd.
doi:10.1016/j.jpcs.2011.03.009

added separately into the mixture in specific mole ratios (with CEAMN/EtOH=0.4 M, $Ti(OBU)_4$/EtOH=0.2 M, $Zr(OP)_4$/EtOH=0.2 M and ACOH/ EtOH=0.05 M) and stirred for 30 min. A small amount of distilled water (about 20 μL) was added to the mixture to accelerate hydrolysis, and CH_3COOH (ACOH) was added to control pH in order to prevent turbidity and precipitation. The pH of the solution was about 4.1. The mixture was then stirred for 24 h. Homogenous transparent solution was achieved. The CeO_2–TiO_2–ZrO_2 solution was aged for 8 days at room temperature (16 ± 3 °C) with a humidity of 50% ($\pm5\%$) to achieve a highly transparent coating. The color of the resulting solution was deep red. Its color was changed to transparent pale yellow during aging, indicating a reduction of cerium (IV) by ethanol [13].

The CeO_2–TiO_2–ZrO_2 thin films were deposited on the Corning glass substrates by the spin-coating technique in a range of 1000–4000 rpm spin speed. The samples were dried for about 1 h at 100 °C after spinning. The process was repeated for three times. The samples were annealed in a temperature controlled furnace at 100 °C for 1 h.

2.2. Sample characterization

To investigate the chemical composition of the CeO_2–TiO_2–ZrO_2 thin films, Fourier transform infrared (FTIR) transmittance spectra were collected from 4000 to 400 cm^{-1} at normal incidence using a FTIR Jasco model 5300 spectrometer. The pH was measured by a Schott–Geraete GmbH CG840 pH-meter. The decomposition and phase transition of the gel was characterized by Differential Scanning Calorimetric–Thermal Gravimetric analysis (DSC–TGA, NETZSCH model STA 409 PC Luxx) up to 600 °C at the scan rate of 20 °C min^{-1} and under N_2 flux. The initial gel was treated at atmospheric pressure with 54% relative humidity and at room temperature (at hydrolytic condition). The CeO_2–TiO_2–ZrO_2 thin film structural characterization has been performed by X-ray diffraction (XRD) using a Philips PW-1840 diffractometer. The diffractometer is equipped with a Cu rotating anode and a monochromator for sample irradiation and detection of the CuK_α radiation scattered from the sample surface. A LEO1430 VP scanning electron microscope (SEM) equipped with Energy Dispersive X-ray (EDX) spectroscopy system, operating under 15 kV voltage was used to determine the cross-sectional morphology information of the films and their chemical components.

The optical transmittance and reflectance of the films in the range from 350 to 800 nm was measured by a 6000 model Aquila nkd spectrophotometer. The refractive index, extinction coefficient, and thickness of the films were calculated by Pro-Optix software. The final values of the refractive index can be fitted to an appropriate function such as the Wemple–DiDomenico dispersion relationship [14,15], i.e., to the single-oscillator model:

$$n^2(\omega)=1+\frac{E_oE_d}{E_o^2-(\hbar\omega)^2}$$

where E_o is the energy of the effective dispersion oscillator and E_d is the dispersion energy.

The morphology study of the films was evaluated in various region using atomic force microscopy (Shimadzu scanning probe microscope, model SPM-9500, Shimadzu Corp.) with a conventional Si cantilever.

3. Results and discussion

The XRD measurements indicate that the sol–gel derived thin films deposited by the spin coating technique are amorphous below 500 °C and no peaks of any crystalline phase of oxide of Ce, Ti, and Zr are observed. These results are in agreement with our previous work [16].

The TGA and the DSC curves of the CeO_2–TiO_2–ZrO_2 gel are illustrated in Fig. 1. Three mass losses are observed. The most important appears between 70 and 110 °C with a mass loss of about 42% followed by two slow decreases between 230–320 and 410–500 °C with the mass losses of 6% and 2%, respectively. At the same time the DSC curve presents at least four important processes: three endothermic at 88, 279 and 428 °C and one exothermic at 492 °C. The first endothermic peak, correlated to the main mass loss, can be related to the withdrawal of the physisorbed water, solvent residues, and unbound stabilizing acid from the material. The second endothermic peak seems to be associated with removing the structural water. The third endothermic peak is relatively slow and steady, ending with a long step on the TG trace, which illustrates that organic solvents have been completely volatilized. The blunt exothermic peak is due to carbonates decomposition releasing carbonyl groups and is correlated to the third mass loss. The exothermic peak cannot be attributed to the crystallization process as confirmed by X-ray diffraction. The differences between our result and Ref. [11] are due to using different routes for preparation of the sol.

Fig. 2 shows the FTIR spectra of the CeO_2–TiO_2–ZrO_2 thin films deposited at three different spin speeds. The broad absorption peak at spectral range 3300–3400 cm^{-1} is typical for porous films

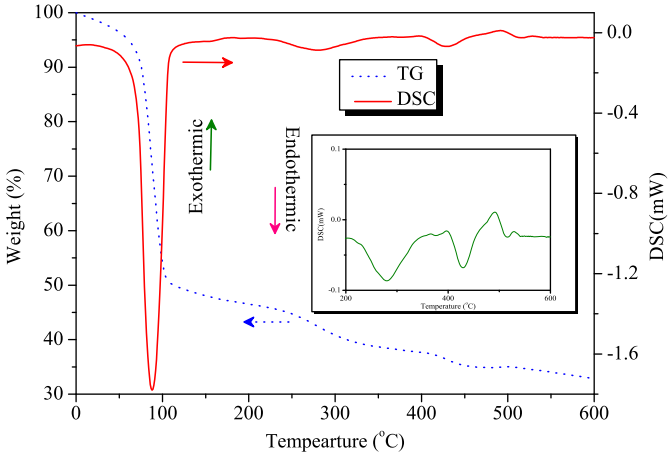

Fig. 1. TG–DSC curves of the gel synthesized by the sol–gel method.

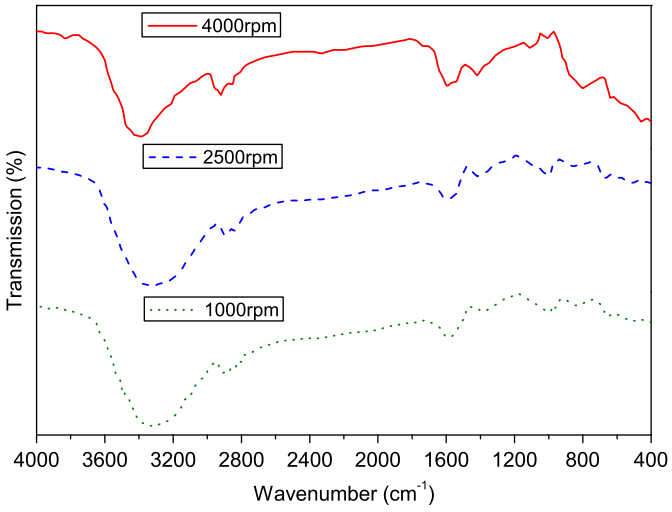

Fig. 2. FTIR spectra of the spin coated CeO_2–TiO_2–ZrO_2 thin films deposited at different spin rates.

and can be attributed to various O−H stretching vibrations of water molecules adsorbed or incorporated in the film structure. Slight variations take place within the samples as their spin speed change. Little changes of the peaks are due to the slight vaporization of water during evaporation stage with increasing of spin speed. The peaks at spectral range 2890–2920 cm^{-1} may be due to the residual NO_2 group and the C–H bonds of the organic compounds originating from the precursor salt, cerium nitrate, alcohol and acid which used in process. The peaks at 1600–1430 cm^{-1} are attributed to Ce=O terminal stretching. The peaks at 990–1100 cm^{-1} can be due to water adsorption. The appearance of the absorption features below 820 cm^{-1} indicates the presence of Ti–O bonds. The Ti–O peak shifted to shorter wavenumbers due to densification of the films with increasing of spin speed. The occurrence of peak at around 690 cm^{-1} is due to stretching vibration and is corroborated to the presence of Zr–O bond. Thus, from the FTIR study, CeO_2, TiO_2, and ZrO_2 phases for the samples are confirmed and thereby samples acquire CeO_2–TiO_2–ZrO_2 mixed composition.

Figs. 3 and 4 represent spectral transmittance and reflectance of the sol–gel derived CeO_2–TiO_2–ZrO_2 thin films prepared by a spin coating technique (1000–4000 rpm) in the wavelength range of 300–1000 nm, respectively. In transmittance spectra, interference fringe bands of the film appeared in the wavelength range of 400–1000 nm for all the films, while reflectance spectra are in the wavelength range of 350–1000 nm for the same films. The amplitude of interference oscillation increased with decreasing spin speed while the depth of interference fringes decreased indicating reduction of thickness of the films with an increasing of spin speed.

The evolution of refractive indices as a function of wavelength for sol–gel derived CeO_2–TiO_2–ZrO_2 thin films deposited at different spin speeds is illustrated in Fig. 5. The refractive index of the films does not conform to a simple rule over the whole wavelength. This may be due to changes of roughness of the surface of the film which causes some fluctuation in the refractive index of the film. This result, in turn, may be due to low viscosity of the sol during deposition that does not a cause change in the structure of the film. Fig. 6 shows the extinction coefficient of the films deposited by the spin coating method using different spin speeds. As can be seen from the figure, similar results have been achieved for the extinction coefficient of the above-mentioned films.

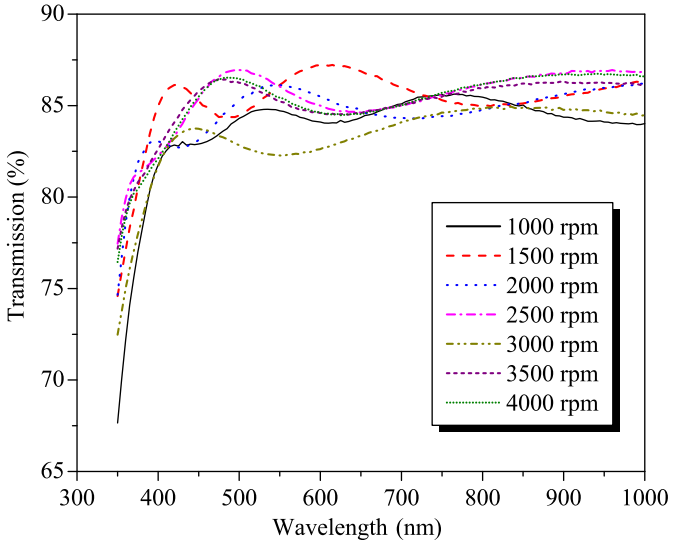

Fig. 3. Spectral transmittance of CeO_2–TiO_2–ZrO_2 thin films deposited by a spin coating technique.

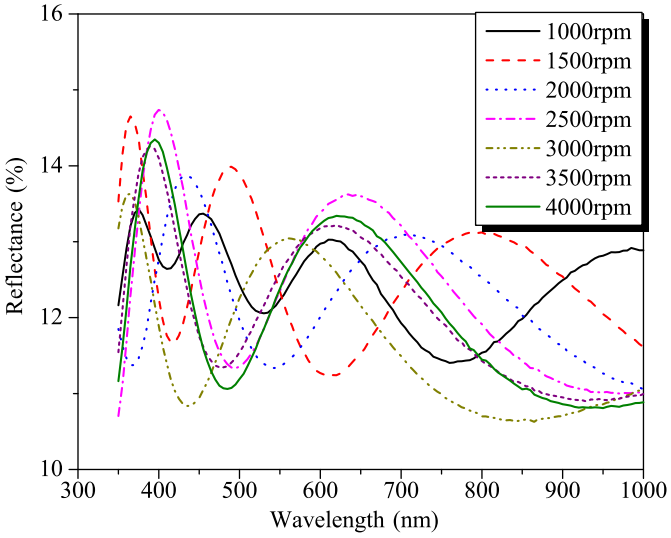

Fig. 4. Reflectance spectra of the spin-coated CeO_2–TiO_2–ZrO_2 thin films prepared by the sol–gel route.

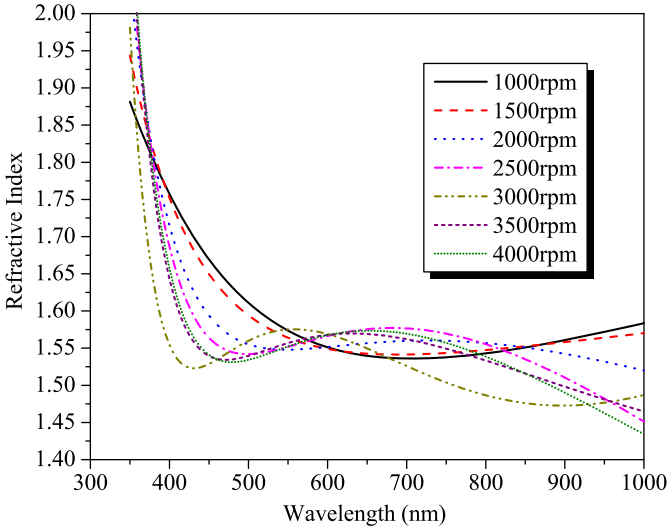

Fig. 5. The refractive index dispersion for the spin-coated CeO_2–TiO_2–ZrO_2 thin films deposited at different spin rates.

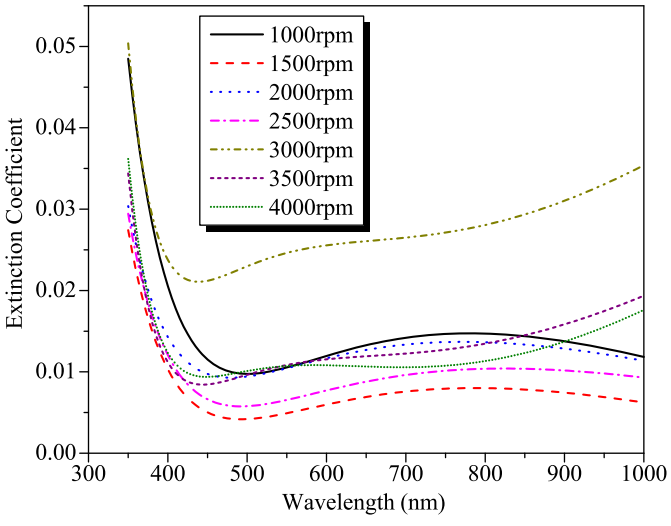

Fig. 6. Wavelength dependence of extinction coefficient for the CeO_2–TiO_2–ZrO_2 thin films deposited by a spin coating technique.

According to Tauc's relationship for the allowed indirect transition, the values of the optical band gap, E_g, are calculated as the intercept of $(\alpha h\nu)^{1/2}$ versus $h\nu$ at $(\alpha h\nu)^{1/2}$ equals zero [17]

$$(\alpha h\nu)^{1/2} = C(h\nu - E_g)$$

where α, C and $h\nu$ are the absorption coefficient, slope of the optical absorption edge and photon energy, respectively.

Fig. 7 shows the plot of $(\alpha h\nu)^{1/2}$ versus $h\nu$ for indirect optical transition of the sol–gel derived CeO_2–TiO_2–ZrO_2 thin films deposited at different spin speeds (1000–4000 rpm). The indirect allowed optical transitions can be determined by drawing a straight line in the strong absorption spectral region [17]. It was found that the optical band gap has the value of $E_g \approx 2.82 \pm 0.04$ eV, independent of the spin rate.

Fig. 8 illustrates the dependence of the thickness of the spin coated CeO_2–TiO_2–ZrO_2 thin films as a function of spin speed. It can be observed that the coating thickness becomes thinner as spin speed rises. E_o and E_d were determined directly from the slope $(E_o\ E_d)^{-1}$, and the intercept on the vertical axis, E_o/E_d by plotting $(n^2-1)^{-1}$ against E^2 and fitting a straight line (Fig. 9). At low energies, a positive curvature deviation from linearity is due

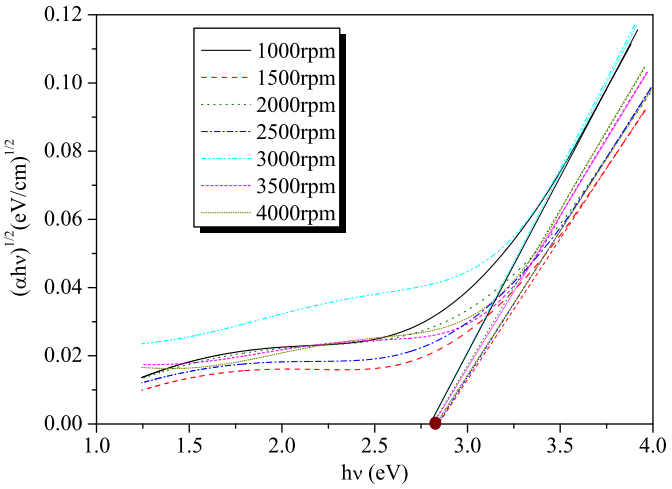

Fig. 7. Plot of $(\alpha h\nu)^{1/2}$ versus $h\nu$ for indirect optical transition of the sol–gel derived CeO_2–TiO_2–ZrO_2 thin films deposited at 1000–4000 rpm spin speed.

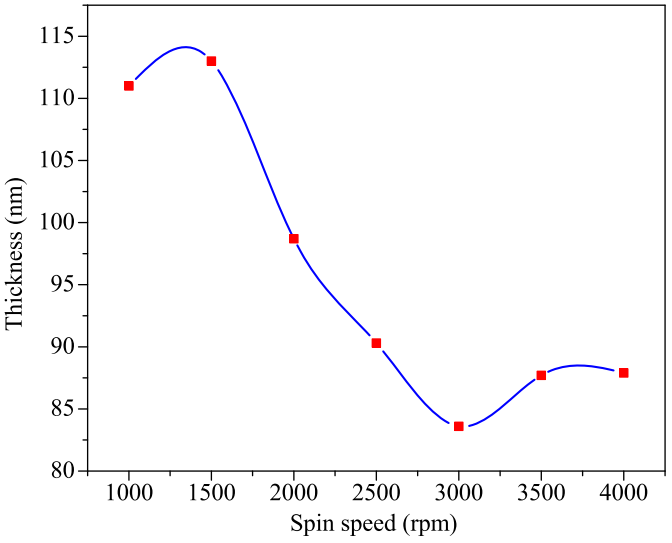

Fig. 8. Thickness dependence of the spin coated CeO_2–TiO_2–ZrO_2 thin films as a function of spin speed.

to negative contribution of lattice vibration to the refractive index and a negative curvature deviation from linearity at high energies is due to the proximity of the band gap edge or excitonic absorption [14]. The values obtained for the dispersion parameter E_o, derived from the above-mentioned equation, were $E_o \approx 5.64 \pm 0.13$ eV. The dispersion energy E_d, were changed from 6.06 to 4.08 eV as spin speed increased from 1000 to 4000 rpm. On the other hand, an approximate value of the optical band gap was also derived from the Wemple–DiDomenico dispersion relationship, according to the expression $E_g^{opt} \approx E_0/2$, obtaining the values for E_g^{opt} of $\approx 2.82 \pm 0.04$ eV. These values show a good agreement with the value obtained from the Tauc's extrapolation [17], using the values of the absorption coefficient calculated from transmission and reflection measurements, as was found above. There is a direct relationship between dispersion energy and cation coordination number [14]. As can be seen in the inset figure of Fig. 9 the oscillator energy is approximately constant for all samples while the dispersion energy decreases with increasing of spin speed. Therefore, the coordination number decreases with spin speed due to increasing of evaporation rate at higher spin speed. The optical band gap energy which is related to oscillator energy is nearly constant.

The surface morphology of the spin coated thin films by AFM is shown in Fig. 10a–d. As can be seen, one can conclude that the spin coated CeO_2–TiO_2–ZrO_2 thin films are dense, pinhole free and nearly smooth. The film deposited at 3000 rpm is flatter. We expect that the roughness of the surface of the film decreases by increasing spinning rate. For the films deposited at 1000–3000 rpm, similar behavior is observed but at 4000 rpm the roughness of surface of the film increases. This may be due to heterogeneous deposition and densification of the film prepared above 3000 rpm. Fig. 11a–c, show the cross-sectional SEM micrographs of CeO_2–TiO_2–ZrO_2 thin films deposited at three different spin speeds (1000, 2500, and 4000 rpm). It reveals that the film deposited at 1000 rpm is less dense, uniform, and smooth with respect to the film deposited at 2500 rpm which is uniform, smooth, and quite dense. On the other hand, the film deposited at 4000 rpm is denser, rougher but less uniform. These tendencies are in good agreement with the AFM results. The thicknesses of the films obtained by cross-sectional SEM confirm the results determined by optical measurements. EDS spectra of the films deposited by using spin coating technique at 1000, 2500, and 4000 rpm spin speeds are given in Fig. 12. As can be seen in Fig. 12, Ce, Ti, Zr, and O elements are present in the films. Si, Na, Ca, and Mg elements which are not expected to be in the films may have resulted from the glass substrates. We think that the change of the film thicknesses and porosities are responsible for the change in Si, Na, Ca, and Mg amounts. In addition, existence of C element in the films may be attributed to residual contamination probably originating from residual C-bonds present in the pore. Also, it was clearly seen that the amounts of C element decrease when the spin speed decreases. The change of C amount with spin speed is in good agreement with FTIR results.

The calculated refractive index, extinction coefficient and thickness of sol–gel derived CeO_2–TiO_2–ZrO_2 thin films deposited by the spin-coating technique in a range of 1000–4000 rpm spin speed are listed in Table 1. The changes of optical constants are in agreement with AFM results. As can be seen, the optical band gap has the value of $E_g \approx 2.82 \pm 0.04$ eV, independent of the spin rate within the limits of error.

4. Conclusion

The low temperature sol–gel synthesis route has successfully led to the formation of spin-coated CeO_2–TiO_2–ZrO_2 thin films. The optical constants (refractive index and extinction coefficient) and thickness of such films were influenced by changing the spin

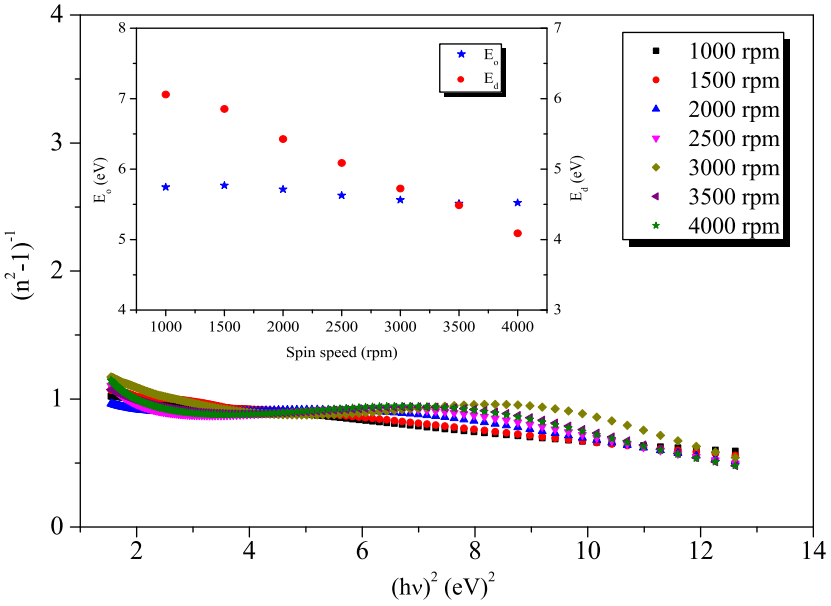

Fig. 9. Plot of refractive index factor $(n^2-1)^{-1}$ versus $\hbar\omega$ for the CeO_2–TiO_2–ZrO_2 thin films. The inset shows oscillator energy E_o, and dispersion energy E_d, as a function of spin speed.

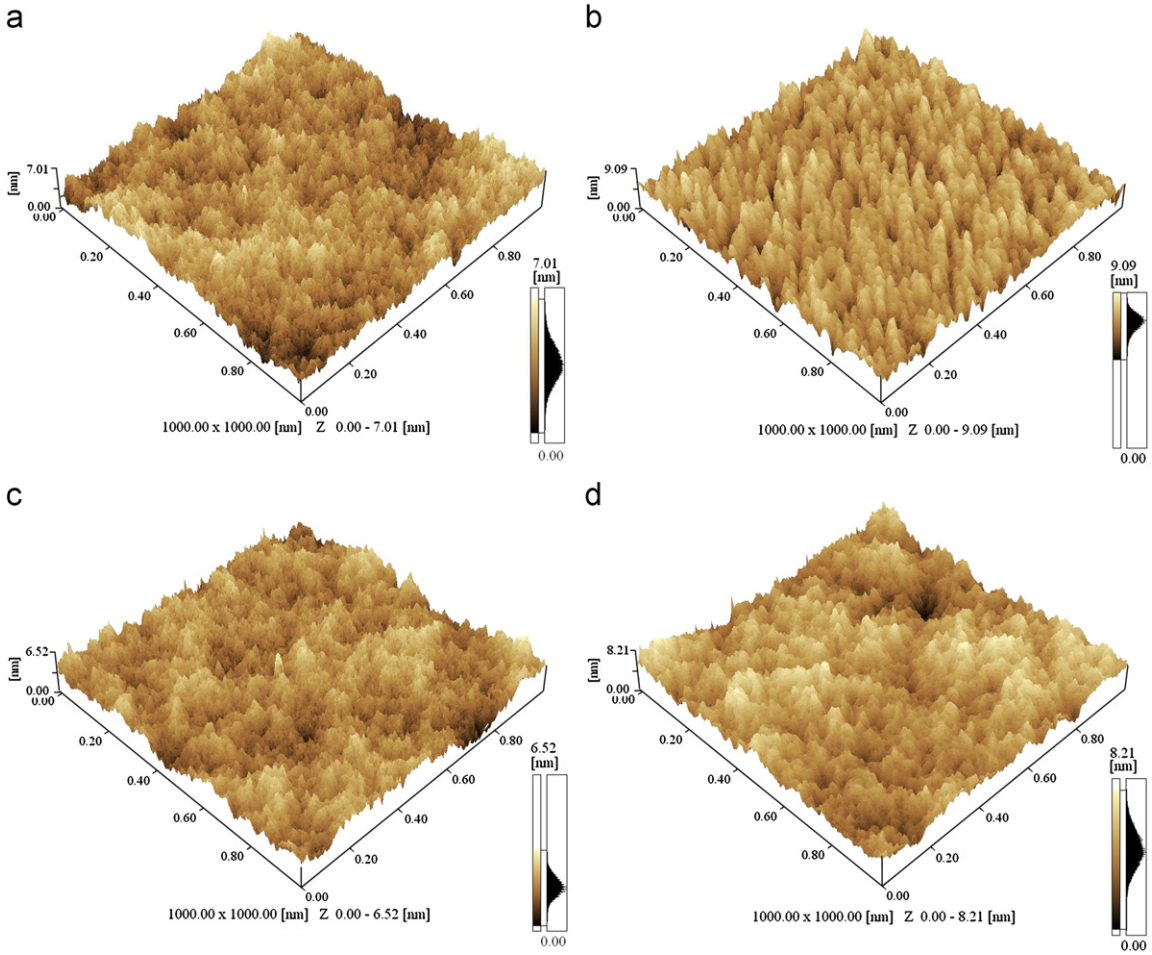

Fig.10. Atomic force microscopy (AFM) images of the spin-coated CeO_2–TiO_2–ZrO_2 thin films deposited on glass substrates at four different spin speeds.

speed. The best result was achieved for the films which were spin coated at 3000 rpm. Furthermore, the sol–gel synthesis route with the spin coating technique was found to be an effective way for producing CeO_2–TiO_2–ZrO_2 thin films which can be good candidates for "smart window" applications [11,16] when optimum physical conditions are present.

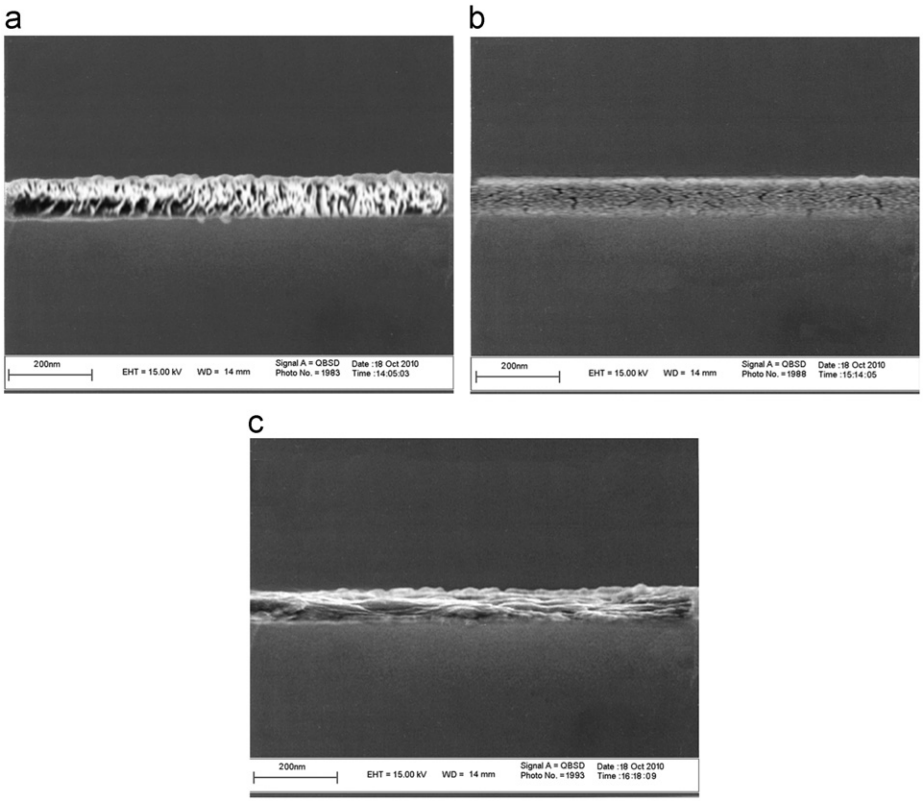

Fig. 11. Cross-sectional SEM images of the spin-coated CeO_2–TiO_2–ZrO_2 thin films deposited at: (a) 1000, (b) 2500, and (c) 4000 rpm spin speeds.

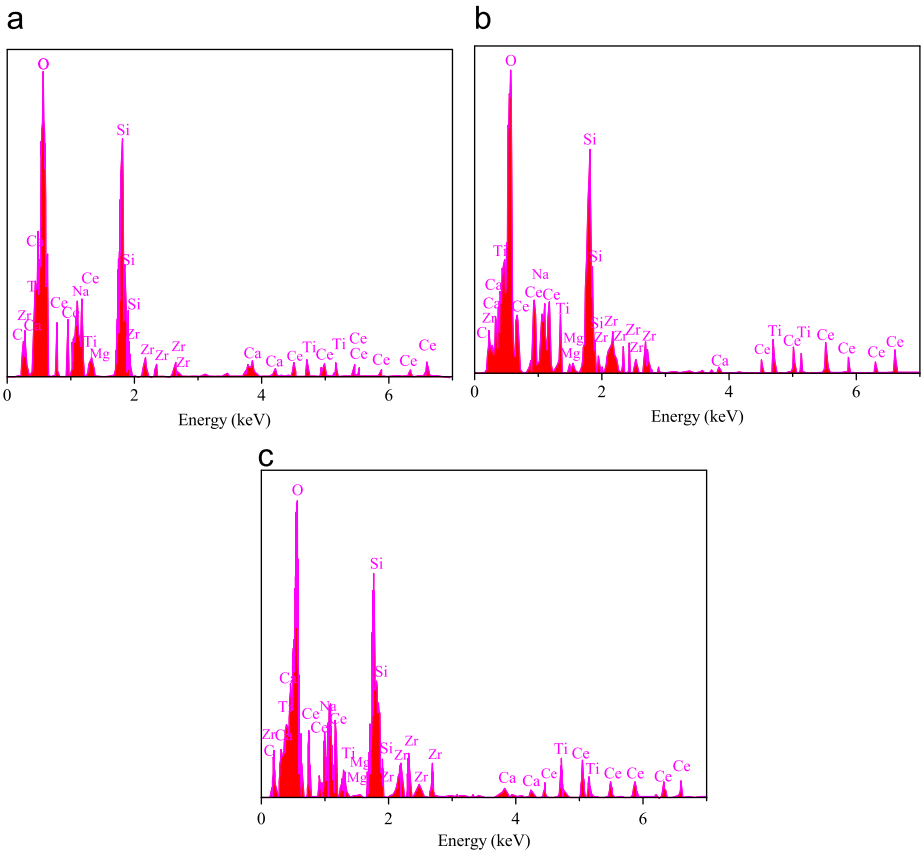

Fig. 12. EDS spectra of the CeO_2–TiO_2–ZrO_2 thin films deposited at: (a) 1000, (b) 2500, and (c) 4000 rpm spin speeds.

Table 1
The calculated refractive index, n, extinction coefficient, k, thickness, d, and indirect band gap E_g of sol–gel derived CeO_2–TiO_2–ZrO_2 thin films deposited by the spin-coating technique in a range of 1000–4000 rpm spin speed.

Sample	ω (rpm)	n (λ=550 nm)	k ($\times 10^{-3}$) (λ=550 nm)	d (nm)	E_g (eV)
1	1000	1.574	10.541	111.0	2.812
2	1500	1.564	5.065	113.0	2.843
3	2000	1.547	10.553	98.7	2.814
4	2500	1.551	6.691	90.3	2.842
5	3000	1.575	24.570	83.6	2.796
6	3500	1.558	10.959	87.7	2.816
7	4000	1.554	10.756	87.9	2.830

Acknowledgement

The authors would like to express their thanks to Prof. Zanjanchi, Department of Chemistry of The University of Guilan for performing XRD measurements, ITU, physics department, thin films laboratory employees for providing AFM and nkd measurements.

References

[1] T.D. Senguttuven, L.K. Malthotra, J. Phys. Chem. Solids 58 (1) (1997) 19.
[2] N. Ozer, J.P. Cronin, Y.J. Yao, A.P. Tomsi, Sol. Energy Mater. Sol. Cells 59 (1999) 355.
[3] F.E. Ghodsi, F.Z. Tepehan, G.G. Tepehan, Thin Solid Films 295 (1997) 11.
[4] S. Mahanty, S. Roy, Suchitra Sen, J. Cryst. Growth 261 (2004) 77.
[5] S. Zhuiykov, W. Wlodarski, Y. Li, Sensors Actuators B 77 (2001) 484.
[6] A. Hagfeldt, N. Vlachopoulos, S. Gilbert, M. Grätzel, SPIE 2255 (1994) 297.
[7] K. Zakrzewska, M. Radeska, M. Rekas, Thin Solid Films 310 (1997) 161.
[8] G. Banfi, V. Degiorgo, D. Ricard, Adv. Phys. 47 (1998) 447.
[9] U. Lavrencic Stangar, B. Orel., I. Grabec, B. Ogorevc, K. Kalcher, Sol. Energy Mater. Sol. Cells 31 (1993) 171.
[10] F.E. Ghodsi, F.Z. Tepehan, G.G. Tepehan, Electrochim. Acta 44/18 (1999) 3127.
[11] Cesar O. Avellaneda, Luis O.S. Bulho\widetildees, Agnieszka Pawlicka, Thin Solid Films 471 (2005) 100.
[12] F. Vassano, F. Decker, E. Masetti, F. Cardellini, A. Licciulli, Electrochim. Acta 44/18 (1999) 3149.
[13] D. Keomany, C. Poinsignon, D. Deroo, Sol. Energy Mater. Sol. Cells 33 (1994) 429.
[14] S.H. Wemple, M. DiDomenico, Phys. Rev. B 3 (1971) 1338.
[15] S.H. Wemple, Phys. Rev. B 8 (1973) 3767.
[16] F.E. Ghodsi, F.Z. Tepehan, G.G. Tepehan, Sol. Energy Mater. Sol. Cells 92 (2008) 234.
[17] J. Tauc, G. Griorovic, A. Yancu, Phys. State Sol. 15 (1996) 627.